2014-06-07

A New Geophysical Strategy for Measuring the Thickness of the Critical Zone

Johnathan R. Yaede
Brigham Young University - Provo

A New Geophysical Strategy for Measuring the Thickness of the Critical Zone

Johnathan R. Yaede

A thesis submitted to the faculty of
Brigham Young University
in partial fulfillment of the requirements for the degree of

Master of Science

John H. McBride, Chair
Stephen T. Nelson
Barry Bickmore

Department of Geology

Brigham Young University

June 2014

ABSTRACT

A New Geophysical Strategy for Measuring the
Thickness of the Critical Zone

Johnathan R. Yaede
Department of Geology, BYU
Master of Science

Estimates of the depth and variation of lateritic weathering profiles are especially important in tropical areas such as Oahu, HI. Shear-wave velocity data were obtained by a new application of Multi-channel Analysis of Surface Waves (MASW) to map the base of the critical zone, to show variations in the LWP, and to derive weathering rates.

The MASW technique proved highly capable of imaging the base of the critical zone, confirmed by lithological well data and direct field measurements. Profile thickness can be obtained without drilling, which has applications in engineering and geochemical studies. The measured rate of advance of the weathering front derived from the thickness measured by MASW ranged from 0.019 m/ka to 0.30 m/ka in mesic zones; about 1500 mm of annual rainfall, while a zone of 800 mm of annual rain fall revealed rates ranging from 0.011 m/ka to 0.013 m/ka. These rates are comparable to geochemically derived rates in previous studies.

Standard p-wave seismic reflection data were insufficient for detecting boundaries as the weathering boundaries are gradational and do not produce reflections. Shear-wave models also showed internal velocity variations that may be caused by weathering heterogeneity due to textural differences in parental lava flows. Soil chemistry revealed the nature of weathering products as enriched in Al, Fe, Ni, and Cr, and commonly contain alteration minerals such as halloysite, kaolinite, maghemite, and ferrihydrite.

Imaging depth limitations were overcome by innovative experiment designs, pushing the boundaries of the current technology. Increasing offsets and combining dispersion curves allowed for a more objective picking of the dispersion curve into the lower frequency domain. Even further improvements were made from a newly developed form of the active/passive technique. These advancements in technology allowed for detailed imaging of the subsurface with greater modeling confidence.

This study showed that velocity models derived from MASW are accurately able to describe laterite weathering profiles in terms of depth and variability, expanding the use of the MASW technique beyond its traditional applications and making it a potential tool of interest for many fields of geoscience.

Keywords: critical zone, weathering front, MASW, laterite weathering profile, Oahu, HI

TABLE OF CONTENTS

Introduction

Tropical volcanic island chains are exposed to severe chemical weathering, especially in areas of high rainfall as is generally true on Oahu, Hawaii, see Nelson et al., 2013 for a recent review. Laterites, or lateritic weathering profiles (LWP's), typically develop in warm, wet regions where chemical weathering is rapid. Warm, moist conditions promote plant growth, leading to high CO2 concentrations in the soil where carbonic acid is consumed in many weathering reactions. Chemical weathering reaction rates strongly depend on temperature (Dixon et al., 2009). These conditions abound on Oahu, Hawaii with significant climate variations across the island (Fig. 1), making this an ideal location to study LWP's due to the presence of mostly a single type of bedrock, tholeiitic basalt.

Chemical weathering has a significant impact on geological materials and thus, on human life. The influence that LWP's have on ground strength, atmospheric carbon dioxide levels (Beaulieu et al., 2012), and on ore deposits, make the study of the critical zone vital. Some have argued that weathering is the most important, yet least studied geologic process (Wilson, 2004; West, 2012). In addition to characterizing ground stability, one of the most important aspects of the critical zone is its thickness as many models stand in need of this parameter for understanding denudation and weathering rates. Measuring the thickness and variability of LWP's can increase our understanding of chemical weathering rates (Hilley et al., 2010). However, estimations of weathering zone thickness is a concern (West, 2012). Hilley et al., 2010). Hilley et al., (2010) stressed that the relationship between denudation and weathering zone thickness is poorly understood. More data from various climatic and tectonic environments are needed in order to better understand this relationship.

One attempt to address the issue of determining weathering zone thickness is to use a derived relationship between erosion rates and relief (Montgomery and Brandon, 2002; Hilley and Porder, 2008), assuming the ground water system may restrict the thickness of the critical zone. While this relationship works well in most environments (Hilley et al., 2010), areas of high relief and extreme chemical weathering rates as are present on Oahu were shown to be incompatible with field measurements. Chemical weathering rates in young rocks with a tropical climate may temporarily out pace erosion rates and lead to a thicker than expected weathering zone. Another complicating factor in ocean island settings is the vertical compartmentalization of shallow circulating groundwater systems that sustain perennial stream flow and deep groundwater systems of the Ghyben-Herzberg lens. In Oahu, these two systems may be vertically separated by hundreds of unaltered rock, where shallow perched systems are more closely related to saprolite development (Nelson et al., 2013).

This study addresses chemical weathering in Hawaiian basalts, or more generally the weathering of intermediate to mafic igneous rocks in tropical environments through critical zone thickness. The focus of this study was to test the ability of Multi-channel Analysis of Surface Waves (MASW) to create a velocity model of the subsurface that can define the base of the critical zone and show variations within the LWP, and to derive rates of advancement of the weathering front. Innovative technological advanced were needed to more accurately model the weathering profile, especially at LWP thicknesses encountered in Oahu. An allied focus was to calibrate the MASW models with geological information from logged wells and geologic measurements, which provide information of the depth of the LWP-bedrock interface.

It is expected that some subsurface boundaries are gradational, such as the transition between saprolite and incompletely weathered basalt, and such boundaries produce diving waves

rather than strong reflections in standard seismic surveys. Diving waves, instead of reflections, prevent imaging of the interface. A non-reflection seismic technique is needed to accurately model the velocity structure of the subsurface.

We investigated 6 sites on Schofield Barracks in the central plain of Oahu (Fig. 2). A LWP outcrop shows the expected variability that the critical zone can display (Fig. 3). Each site is overlain by a thick LWP that overlies mostly unaltered basalt. LWP thicknesses in some cases can be constrained with relatively high precision due to the presence of nearby wells with geologic logs, or by outcrop. In all cases, LWP thickness is consistent within a general range based upon compiled geologic logs. As a comparison case, we have also investigated an arid site near Fillmore Utah (Fig. 4).

Importance of Laterite Weathering Profiles

Climate and Weathering Rates

The thickness of the LWP varies with climate conditions, reflecting weathering rates. Tropical volcanic islands are ideal for studying the effects of climate on denudation as there are significant climate variations, but little variation in other factors that may affect erosion rates, such as lithology and tectonic deformation (Ferrier et al. 2013, Nelson et al., 2013). Where vigorous weathering is present as is on parts of Oahu, the LWP acts as a major sink for atmospheric CO2. Weathering in young volcanic arcs and ocean islands represents as much as 30% of the atmospheric CO2 sink (Dessert et al., 2003).

The drawdown of atmospheric CO2 by chemical weathering of silicates as CO2 concentrations rise is significant. Beaulieu et al. (2010) simulated this consumption to be about 3% per 100 ppmv rise in CO2. Lenton and Britton (2006) used a model that predicted it would take about 1 million years for silicate weathering to stabilize atmospheric CO2 levels. In the

Mackenzie River basin, one model inferred a rise from 355 ppmv to 560 ppmv by 2100 captured 50% more CO2 through chemical weathering, 40% of which is attributed as a direct result of climate change (Beaulieu et al., 2012).

At a geologic time scale, this suggests that the earth climate naturally stabilizes. Several other authors have argued that major global climate changes have occurred because of changes in the rate of chemical weathering (Arthur et al. 1998; Cohen et al 2004; Pearson and Palmer, 2000; Kump et al. 2000; Raymo, 1991). During increased continental exposure, the increase of chemical weathering rates may have contributed to glaciation that occurred during the drawdown of CO2 (Kump et al., 2000). Several have argued that the late Cenozoic ice age was in response to the orogenic events that formed the Himalayas and Andes, exposing vast amounts of material available for chemical weathering (Raymo, 1991, Kashiwagi et al., 2008; Zachos and Kump, 2005).

In spite of these arguments and findings, there remains much uncertainty about the relationship between CO2 drawdown and chemical weathering (Goudie and Viles, 2012; West 2012). Obviously, more work is needed to understand the link between weathering and global carbon cycles. Studies and data on chemical weathering rates from a variety of geologic settings from around the world are needed in order test hypotheses on the major controls of weathering rates and their relationship to the long term carbon cycle (Goudie and Viles, 2012). Paramount to these studies would be a better understanding of the relationship between denudation rates and critical zone thickness, and how thickness varies in different climate settings (Hilley et al., 2010).

The purpose of this study is to provide needed research on the determination of the weathering zone thickness at a local scale, which can lead to a greater understanding of chemical weathering rates as a function of climate. The methodology presented in the report may be

regarded as a valuable tool to researchers interested in understanding how weathering varies in the subsurface in many geologic settings.

Economic Value

The weathering of ultramafic rocks concentrates metal such as iron, aluminum, gold, niobium, and phosphorus (Freyssinet et al., 2005). With a decline in Ni-bearing sulfide lode deposits (Dalvi et al., 2004), there is a need to develop alternative sources of Ni. LWP's provide one of these alternatives and have been given growing attention (Marsh and Anderson, 2011). Bauxites (Al-rich laterite), of potential ore in Hawaii represent nearly all mined Al deposits (Bell and Ho, 1996).

The quality of the ore deposit depends on the composition of the protolith and on climate conditions that can facilitate elemental leaching, and therefore concentrate the least soluble elements (Gleeson and others, 2003, Younge and Moomaw, 1960). Oahu's wet climate regions allows for weathering conditions that remove mobile elements like K, Ca, Na, and Mg while enriching Ti, Al, and Fe. These weathering products include commonly found aluminosilicates, halloysite/kaolinite $Al2Si2O5(OH)4$ and the iron oxide maghemite $Fe2O3$ (Nelson et al., 2013). More deeply weathered material contains the aluminum hydroxide, Gibbsite $Al(OH)3$, which is the principle mineral found in bauxite deposits (Patterson, 1967). Meyer et al., 2002 showed a similar trend of kaolinite and gibbsite formation in granitic laterites. Rapid chemical weathering conditions make the study of LWPs on Oahu valuable from both economic and process level perspectives.

Explorations for potential buried laterite deposits have commonly used geophysical techniques such as magnetic, gravity, electromagnetic, electrical and ground-penetrating radar (Marsh and Anderson, 2011). The use of MASW is a quick and relatively inexpensive method

and may provide a more detailed model of the subsurface, identifying zones of heavy weathering that produce bauxite deposits. While bauxite deposits on Oahu are currently of little interest, deposits on other Hawaiian islands, especially on Kauai, are of more significant commercial interest (Younge and Moomaw, 1960). The older age of Kauai and the more extensive rainfall, creates thick, concentrated blankets of bauxite ore.

Engineering & Seismic Considerations

Severe chemical weathering affects the mechanical properties of the laterite. In heavily populated tropical regions like Oahu, these effects are of particular interest when considering the design of roads or structures, and when seismic safety or ground stability is of concern. The shear strength of the laterite can be highly variable due to variations of Fe-minerals acting as a cement, as well as water saturation (Chandrakaran and Nambiar 1993; Gui and Yu, 2008).

While having a relatively homogenous rock type, variations in the texture of lava flows can affect the degree weathering has weakened the laterite. Sirles (2013) found that the variations of depth-to-bedrock on Oahu were larger than expected, and that significant lateral heterogeneity in weathering was found during a site evaluation for road construction. MASW provides a low-cost, non-invasive means of investigating the subsurface (Xia et al., 1999, Hunter et al., 2002). It can eliminate the need for excessive use of boreholes that are often costly.

MASW

Multichannel analysis of surface waves, also known as MASW (Park et al., 1999), has become widely used as a geophysical technique to estimated shear-wave velocities in the near-surface environment over the past 2 decades (Zeng et al., 2012). Its popularity has grown because of its effectiveness for providing shear-wave velocity measurements, and because it is easier to use than other seismic approaches (Park, 2013).

In any seismic approach, surface wave energy dominates the seismic shot record with Rayleigh waves make up more than two-thirds of the total energy generated, and it is considered noise in traditional seismic techniques (Richart et al. 1970; Xia et al., 2002). Surface and guided waves are commonly regarded as interference needed to be filtered from the seismic record (Boiero et al., 2013). However, the dispersive properties of the surface waves allow for elastic properties of soil and rock to be inferred, and a shear wave velocity profile is obtained from analyzing a dispersion curve of the fundamental-mode (Park et. al 1999), making these waves useful to near-surface geophysical applications (Boiero et al., 2013).

Often, shear-wave velocity data are estimated for ground response modeling (Hunter et al., 2002) as shear-wave velocity information is a good indicator of material stiffness (Park, 2013). MASW provides a way to directly measure shear-wave velocity and provide better data for ground response models then a mere estimate. Traditional use of cross-hole or down-hole shear-wave velocity measurements are expensive and can miss vital information about the horizontal distribution of the shear-wave velocities that affect ground strength (Sirles et al., 2013, Kaufmann et al., 2005). Trupti et al. (2012) used shear-wave velocity measurements from MASW to characterize a site in Andhra Pradesh, India according to seismic hazard assessments. Eker et al. (2012) performed a seismic zonation study using the MASW method Ankara, Turkey. Mahajan (2008) measured the shear-wave velocity of alluvial sediments to find Vs 30 measurements in the sub Himalayan mountain city of Dehradun.

The effectiveness for MASW to give an accurate measure of shear-wave velocity has been well established. Banab and Motazedian (2010) showed the effectiveness of using MASW to obtain a shear-wave velocity profile in shallow, loose soil layers by comparing the data with borehole data. Boriero et al. (2013) has shown its effectiveness by comparing MASW velocity

data to reflection and borehole data. Eker et al. (2012) showed that the MASW derived soil profile compared well to conducted geotechnical borings. Karray et al. (2009) showed how MASW compared well with cone penetration tests and standard penetration tests to evaluate sediment compaction performance during dam construction in Quebec. Kaufmann et al. (2005) showed MASW Vs measurements agreed within 15% error to borehole measurements. While the effectiveness of MASW to give an accurate measure of shear-wave velocity model in many different geologic conditions has been well established, applications beyond traditional engineering studies are sparse.

Most applications to date have been with regards to civil engineering and more specifically measurements of shear-wave velocity of the upper 30 m, but applications have expanded into other area of study. MASW has been used to map the bedrock/soil interface (Sirles et al., 2013; Choon 2013; Trupi et al., 2012; Carnevale et al., 2005; Karray et al., 2012). Watabe and Sassa (2008) used MASW to successfully identify tidal flat stratigraphy in Japan. Kaufmann et al. (2005) used MASW in a submarine setting, identifying anomalous areas that borings missed of the eastern coast of Florida. The MASW methods has also been successful at landfill sites to aid in developments, improvements, and remediation (Suto, 2013; Suto and Lacy, 2011; Suto and Cenic, 2012). Near-surface cavities are also identifiable through MASW (Karray and Lefebvre 2009; Xu and Butt, 2006).

On Oahu, one study employed MASW to understand the near-subsurface in preparation for the construction of a mass transit system (Sirles et al., 2013). From initial borings engineers were surprised by 1) the existence of soft soils, 2) a highly variable depth to bedrock, and 3) depth to bedrock exceeding the predicted 30 m. As a result, a continuous geophysical evaluation of the subsurface was needed along the transit system alignment. Due to noisy condition along

the highway, a passive MASW method was employed (Park and Miller, 2008), where the depth to bedrock modeled by the surface-wave analysis was within 5% of that encountered by the borings. The successful use of MASW combined with correlation to borings allowed mapping the depth to mostly unaltered bedrock over a large continuous area.

Geologic Setting

Oahu, HI

The island of Oahu is dominated by two large shield volcanoes, the 3.2 to 1.8 Ma Koolau volcano to the east and the 4.0-2.6 Ma Waianae volcano to the west. The western side of the Waianae volcano and the eastern side of the Koolau volcano have collapsed into the ocean, with the remaining island being constructed of their overlapping remnants (Sherrod et al., 2007, Nelson et al., 2013). The survey sites are located on the central part of the island on smooth, flat plains located between the two volcanoes. The area is deeply incised by numerous streams.

Theolitic basalt is the dominant rock type, and the lithologic homogenous nature of the island makes this an ideal location to study weathering. While bedrock is homogenous, there are variations in flow types between ‘A’a and pahoehoe. Climate conditions on Oahu vary significantly and result in a wide range of LWP thickness. Annual precipitation varies by more than an order of magnitude on Oahu (Lau and Mink, 2006). Our main profiles lie within a mesic climate zone, averaging about 1500 mm of annual rainfall (Fig. 1). Monitoring wells with geologic logs located near our survey areas suggest LWP ranging in thickness from ~30-50 m.

Reference Site at Ice Springs, Utah

The Ice Springs survey site near Fillmore (Fig. 4) is comprised of unweathered Quaternary basalt flows with overlying Quaternary sediments. These basalts are mostly unweathered due to the semi-arid climate, mean precipitation being <230 mm/yr. A driller’s log

from an adjacent well reveals that valley fill sediments is ~ 5m thick over ~26 m of Quaternary basalt. We confirmed the depth to the top of the lava with a hand-augured hole at 4.67 m.

Methods

Seismic

As mentioned above, this study employed Multi-channel Analysis of Surface Waves (Park et al., 1999). The data acquisition involved multichannel shot gathers similar to conventional common midpoint (CMP) reflection surveys. An innovative active survey method and a combination active/passive methods were used in order to establish a best practice to improve depth of investigation.

Both experiments setups used a 7.25 kg sledge hammer source with 24 or 48 active stations. Vertically spiked, low frequency geophones (4.5 Hz) were used. These surveys used a one fixed source offset moving into the receiver spread 24 times by 1dx (1.5 m) between each shot station to generate a 48-channel roll-along record. The other experiments used 24 active station roll-along method with the same source geometry.

Active Survey

For the standard active survey, the initial source to receiver offset (X1) was set at 10.7 m with 3 gathers stacked at each station. The source was then advanced at 1.5 m (dx) increments for a total of 25 stations. The recording time was set at 2 ms with no acquisition filters. After initial experiments failed to provide the needed depth of investigation, a new strategy of using increased multiple offsets and combining their respective OT images was explored. This allowed for dispersion curves to be picked into the lower frequency domain with less subjectivity and greater confidence. For 3 of the survey areas (line 3, line 6, and Ice Springs), 3 addition offsets

were employed at 21.3 m, 32 m & 42.7 m. The other 3 areas used only 2 addition offsets. Experiments were run with the same acquisition parameters.

Processing

Data were processed using SurfSeis software developed at the Kansas Geological Survey. The processing steps are as follows: 1) Data Acquisition in SEG-2 format, 2) Data Conversion into KGS format, 3) Encoding Field Geometry, 4) Dispersion Imaging, 5) Dispersion curve Extraction, and 6) Inversion. Due to our unique field set for improving the depth of investigation potential, some alterations to the tradition processing steps were needed.

Each offset was initially treated as a separate experiment until the dispersion curve extraction step. The dispersion image was generated by transferring the shot gather into the frequency-domain. The four dispersion images, one from each offset (with the same active phone geometry during acquisition), were then combined. This final image was used to determine the appropriate extraction of the fundamental mode of the Rayleigh wave by tracing the high energy concentrations on the combined dispersion images. The Vs profile was then calculated using a normal iterative inversion process.

Passive/Active Survey

In an attempt to find another strategy for increasing the depth of investigation, a new mixed passive/active survey technique was developed. The experimental setup was similar to the active survey design. However, in this case the initial source receiver distance was set at 18.3 m. At each source station an initial strike triggered the recording. The recording time was set to 60 seconds with a sample rate of 4 ms and no acquisition filters. During the 60 second recording

time another strike occurred every 5 seconds, moving back 1.5 m between each strike. 25 records were acquiring moving forward 1.5 m between each record.

The processing scheme was based on the utilization of the several MASW techniques developed for both active and passive surveys. It first adopts the technique (Park and Shawver, 2009) that can process surface waves generated at multiple source offsets that aims at minimizing the harmful near-field effects of surface waves. This multi-source-offset technique is known to increase accuracy of surface-wave analysis in a broad depth range of investigation (Park and Carnevale, 2010). The processing scheme also used the technique that can dynamically detect the source characteristics (i.e., angle and distance) from the continuous scanning of surface waves for a wide range of azimuth (Park, 2008). The technique, however, used only two opposite azimuth angles of +/- 180 degrees based on the inline surface wave propagation as suggested by Park and Miller (2008) that is valid for the linear receiver array.

Geologic Controls

Well data were obtained with help from Steve Turnbull, Hydrologist at the DPW Environmental (ERDC/WES Contractor) stationed at Schofield Barracks, HI. One well log was obtain from the USGS. These well logs gave relatively detailed stratigraphic information from cuttings during drilling. The top of mostly unweathered basalt was based on a description of rigidity and transition from reddish orange color to olive gray to black of the cuttings. While there was no well data directly beneath a profile there was well control close to two survey locations and several wells in the same general area that shed some light on total variability in LWP thickness. Road cut control was also available for one survey location.

Mineralogy & Geochemistry

Soil/saprolite samples give a generalized description of subsurface mineralogy to give geologic context of material imaged (Fig. 3). While any data directly beneath a survey line were unavailable, the results were expected to give a reasonable view into what we would expect to find in a borehole. Surface samples from across the island were analyzed in terms of elemental leaching and qualitative clay mineralogy to give a sense of what elements have formed under various climate conditions. It is expected that variations due to climate across the island will have similar effects in vertical section as various parts of the critical zone have different exposure to groundwater over geologic time.

In order to write weathering reactions, the mineralogy of fresh basalt and altered material must be understood. The mineralogy of weathered sample were determined at Brigham Young University using a Scintag XDS 200 X-ray diffractometer. XRD data were reduced using RockJock (Eberl, 2003) in order to infer mineralogical abundances. In order to determine the elemental mobility during weathering, whole rock chemistry was required for a suite of surface samples. Whole rock major element and trace element chemistry was determined by X-ray fluorescence analysis using a Rigaku ZSX Primus II spectrometer. The composition of each mineral phase present in a typical Oahu tholeiite was determined by electron probe micro-analysis (EMPA) using a Cameca SX 50 electron microprobe at BYU.

Results

This study shows the MASW velocity models for each of our sites. It also compares the results for single offset, combined offsets and the new passive/active strategy. Geologic constraints from well data and measure section are discussed where applicable, and the chemical

analysis of our samples is presented. Rates of the advancement of the weathering front are also estimated. Overall seismic data quality were good. Signal to noise ratios generally fell from the high 80% - mid 90%. Shot records showed clear and nearly ideal surface wave dispersion (Fig. 5).

Multiple offsets

The combination of multiple offsets provided dramatic improvement on dispersion images in the low frequency domain and hence on depth of investigation. Dispersion images from line 3 show this improvement (Fig. 6). The other sites show similar results. This new strategy allowed for a more obvious and objective picking of the dispersion curve and resulted in a greater investigation depth for the models. This improvement was as much as 20 meters increased depth in some cases. No use of a signal long or short offset provided a model sufficient for the investigation of the zone of interest, but the combination of offsets created a powerful experimental design for improving the modeling capability of the MASW technique in terms of depth.

Active/Passive

The active/passive method used in this study also overcame the problem depth limitations to a higher degree. This method was employed at two sites, line 3 and line 6. Although requiring more physical effort, the results were valuable for increasing the depth of investigation.

Reference Site: Ice Springs, Utah

This site was chosen for initial tests on the ability of MASW to investigate a basalt overlain by lower-velocity material and to give a reference site for comparison on Oahu, HI. By contrast to Hawaii, the dry climate of Utah has resulted in little to no chemical weathering of the

bedrock such that the interface between basalt and valley fill is sharp. Geochemically, the basalts from this location and Oahu, HI are very similar and should display a similar shear wave velocity measure.

A drillers log from a nearby water well shows a depth to bedrock of 4.5 m while a hand augured hole on the survey line showed marl down to bedrock at 4.67 m (Fig. 7). These data correlate very well with our seismic velocity model derived from the combination of 4 offsets. The velocity for this boundary occurs at ~ 500m/s (Fig. 8).

Using only a single offset at 10.7 m we were able to image the depth to bedrock, but only a few meters below. With the combination of the 10.7 m, 21.3 m, and 32 m offsets the experiment was able to increase the depth of the model, but it still did not reveal the bottom of the lava flow. Adding a fourth offset at 42. 7 m permitted the picking of a high confidence dispersion curve that increased our model to see beyond the lava flow and into what is likely to be more valley fill sediments.

Line 1 & 2

Lines 1 and 2 did not provide sufficient sounding depth to create confident models of the subsurface. Line 1 was located near line 3 (Fig. 2), but was closer to the road were noise levels from traffic produces poor quality seismic data. Line 2 was only acquired with only the combination of 2 offsets and did not give sufficient data for the purposes of this study.

Line 3

Initial experiments proved to be insufficient, probing a depth of only 18 m. This resulted in no velocity gradients or absolute velocities comparable to our reference site, suggesting that the depth of penetration was poor. The combination of the 4 offsets produced significant

improvements, and gave enough depth to image suspected mostly unaltered bedrock below about 25 m (Fig. 9). The apparent bedrock boundary varies between 26 m-34 at the ~500 m/sec velocity, as inferred from the reference site. This agrees well with nearby well data (Fig. 7). There is a subtle velocity inversion around 15 m, which may be a result of original textural differences between lava flow types where mineralogical variations can give difference seismic velocities.

This site also implemented the active/passive method (Fig. 10). This dramatically improved the depth of investigation to ~76 m. Assuming the bedrock to be 500 m/sec, this places the depth to bedrock at about the same location as the 4 offset model. However, the boundary is better resolved and further depth is shown. This model also infers internal variation of the critical zone.

Well data from the area shows similar overall internal variably (Fig. 7). The nearest well shows depth-to-bedrock at about 33 m and is within 30 m of the profile. A well located about 200 m away shows a thicker depth of about 40 m.

Line 4 and Line 5

These two lines were located about 100 m apart and show similar depth-to-bedrock around 36 m, but contain variable internal velocities within the LWP (Fig. 11). In fact, one model showed almost no velocity inversions or lateral variability whereas the other showed a large inversion and also significant lateral variability. This suggests that velocity difference in the critical zone can occur over rather short distances. These interfaces also fall within the range of expected depths to basalt as suggested by the well data.

Line 6

This experiment was conducted on a dryer part of the island; about 800 mm mean annual rainfall versus on The U.S. Army Schofield Barracks, which receives more than 2,000 mm per year. The critical zone should be significantly thinned due to climate differences. At 500 m/s there is a boundary correlating to a depth about 15 m. Both the active/passive and the combination of 4 different offsets show boundaries at the same depth (Figs. 10 & 12).

This area provided an opportunity to directly measure the depth to unweathered bedrock with two geologic constraints: well data and a measured section. The USGS well data showed the depth-to-bedrock at 20 m. Our survey line was ~5 m below the top of the hill where the well is located. A measured section along a road cut in a nearby highway gave a similar thickness of ~20 m, also starting 5 m higher than the survey location. Both MASW experiments proved to correlate very well with geologic constraints.

Weathering Rates

Weathering rates were calculated based on observed depth to bedrock from wells, measured section, and shear wave velocity models divided by the youngest age for Koolau volcano (Table 1). The youngest age was used because profiles were run on the flat surfaces on the inward part of the island that have not collapsed into the ocean. This area is a relatively undisturbed area dissected by streams. The reasonable assumption that there is no aggradation from sediment accumulation was also made.

The range for rate of advancement of the weathering front on Schofield Barracks is between 0.019 -0.030 m/ka. Weathering rates calculated from Mink Park show a slower rate of advancement of the weathering front between 0.011-0.013 m/ka. The Mink Park location

receives 800 mm of annual rainfall while the Schofield Barracks location receives 1500 mm of annual rainfall. Under the assumption of rates derived from the oldest age, weathering rates range from 0.011 - 0.017 m/ka on Schofield Barracks and 0.006 – 0.008 m/ka at Mink Park.

Geochemical Data

To help give a better geologic context and eventually investigate the possible impact of the degree of weathering and chemical leaching on shear wave velocity, we have taken several saprolite samples in measured section and analyzed them using RockJock (Erberl, 2003) for quantitative mineralogy. Mineral concentrations under 3% were ignored. The mineralogical differences show how significant these variations can be. We also obtained a more detailed chemical analysis of surface samples across the island in different climatic zones.

LWP Samples

XRD analysis determined how the mineralogy of Oahu tholeiites (Plagioclase, Orthopyroxene, and Clinopyroxene) change with weathering. Moderately altered samples were dominated by kaolinite, halloysite, and illmenite. More heavily altered products contained halloysite, illmenite, and maghemite. Samples showing the highest degree of alteration were dominated by gibbsite, maghemite, and goethite.

Figure 3 shows an outcrop of the LWP created during airfield construction on Schofield Barracks during World War II. The XRD analysis reveals the composition of each sample and shows how the degree of weathering is variable both vertically and laterally in a short distance (Fig. 13). A similar analysis on samples near Mink Park reveal a lesser abundance of halloysite and iron oxides with a greater abundance of kaolinite. The general analysis of weathered material shows an abundance of kaolinite and halloysite, with gibbsite forming as weathering becomes more dramatic. One sample on the north side of the island contained 8% quartz.

Surface Samples

Major element XRF analysis determined the mobility of specific elements during weathering of Oahu tholeiites. Specifically, major element analysis revealed that weathering on Oahu removes Si, Mg, Ca, and Na while enriching Al, Ti, and Fe compared to a typical mostly unaltered Hawaiian theoliite, sample HWN-68 (Table 2; Fig. 13). A simple weathering classification can be based on the amount of Si left in a sample compared to the relative enrichment of Al, Ti, and Fe.

Slightly altered samples show a SiO2 concentration of ~50 wt % while moderately weathered samples drop to ~35 wt % SiO2. Severely weathered samples drop to ~10 wt % SiO2. Sample 1 is a slightly altered sample based on its retention of most of its SiO2. It contains kaolinite and halloysite. Its geologic description is a mildly altered vesicular basalt, original texture entirely intact but phenocrysts have been replaced (ghost phenocrysts), gray in color on fresh surfaces, altered edges brown to black, hard. More severely weathered samples contain no original texture, phenocrysts, or vesicles, and their colors are commonly deep brown and red. The degree of weathering can also be seen by Al, Ti, and Fe enrichment as more heavily altered material have greater abundances of these elements, seen most dramatically by sample 8 (Fig. 14)

Sample 6 is a moderately weathered sample based on SiO2 depletion, Al and Fe enrichment, and physical description. The sample reveals that kaolinite and halloysite are the dominate clays, and iron oxides present. The results are similar with all the moderately weathered samples. Sample 8 is a much deeper weathered material with most of its SiO2 having been removed. Strong gibbsite peaks were observed and confirmed with heat treatment that destroyed the gibbsite clay peaks. The same mineralogical and leaching conditions that exist

across the different climate zones are likely to be the same differences that exist down section in the LWP due to groundwater contact time.

Discussion

The results of the MASW methods show that an accurate model of the subsurface within a lateritic weathering profile of significant thickness can be obtained with proper acquisition parameters and improved data handling strategies. Geologic constrains from well and outcrop data provides correlations that confirm interpretations from the MASW models. The reference site in Utah gave 100% certainty of the depth of the basalt and correlated very well to the MASW data. Experience at the reference site guided interpretations in Oahu, including establishing a Vs threshold for mostly unaltered basalt. Showing the accuracy of the MASW method to map the bedrock where saprolite and velocity inversions exist gives confidence to expand the method to areas that lack geologic constraints.

The measured velocity of bedrock from the MASW method differs dramatically from the expected velocity of unweathered basalt. In spite of this, there is consistency within the MASW models that gave similar velocities for each area. A higher mode analysis is needed in order to obtain accurate Vs measures of bedrock (Casto et al, 2010). While not yet examined in great detail, dispersion trends at the highest frequencies in some field records (e.g., 100-125 Hz) indicated bedrock may have shear-wave velocity as high as 3,650 m/sec, which is comparable to expected velocity measures for basalt.

Velocity models and well data show that dramatic changes in the critical zone can occur over short vertical and horizontal distances. This shows the danger in using a point source for a full description of the subsurface. Ground stability and seismic hazard assessments can be

obtained with greater detail using MASW over traditional seismic methods or point sources such as wells or bore holes.

The rates of advancement of the weathering front compared well to the rates previously established using Si-flux indexing (Nelson et al., 2013). The dryer climate conditions from Mink Park result in a slower rate of weathering compared to the wetter climate of Schofield Barracks. This correlation is likely to exist across the island as climate conditions are extremely variable and may be confirmed with further experimentation. A quantitative correlation between rainfall and measured rates of the advancement on Oahu from MASW may be possible to establish with further study.

While the thickness of the critical zone is vital for understanding weathering rates and potential climate implications, geochemistry can further our understanding of the weathering processes. The surface soil geochemistry shows how weathering products vary with climate across the island. Mineralogy can increase understanding of the degree of weathering and the degree to which immobile elements are concentrated. This study confirmed an expected negative correlation between Fe and Al with Si. This negative correlation may aid in the application of geophysical techniques for bauxite exploration (Laskou and Economou-Eliopoulos, 2013). MASW data from this study suggests that this may be possible on Hawaiian Islands.

With the knowledge obtained from XRD analysis, a clay production weathering pathway of; Hawaiian tholeiitic basalts → kaolinite/halloysite → halloysite/iron oxides → gibbsite is seen. Samples from the relatively wet climate zone on Schofield Barracks showed more advanced weathering products than those found at Mink Park under dryer conditions. Dryer areas

contain principally kaolinite and halloysite, and in some cases of very low precipitation zones, no clays are present.

The sample from the north side of the island is unique from other samples due to the abundance of quartz. This sample was taken from a road cut of freshly exposed saprolite. It is unlikely that the quartz is eolian derived but is most likely to result from a silica rich groundmass as the sample has not been exposed to the atmosphere, and the quartz is not widespread among samples across the island.

Down section mineralogical differences are likely a result of varying degrees of ground water contact due to textural differences from flow types. This is consistent with Sadleir and Gilkes (1976) who observed two different protoliths leading to a similar gibbsite rich lateritic bauxite deposit; the major control being textural differences between rocks and not mineralogy due to different rock types. Some models show velocity variations and inversions that may correlate with this heterogeneity of weathering productions as seen on figure 3 and makes MASW a potentially useful tool for identifying features of interest.

An important future study would be to determine the shear-wave velocity, as measured by MASW, of the different degrees of weathering. This could lead to the identification of important ore targets and reveal important information for engineers as more heavily weathered material has less elastic strength. This study has not investigated if a direct correlation to apparent subsurface features is possible using MASW. In order to explore this problem drilling is needed to establish the character of subsurface targets.

The depth to basalt results confirms an expected positive correlation between rainfall and weathering. The study area in Utah receives little rainfall and results in unweathered basalt at very shallow depths. On Schofield Barracks there is significant weathering with thick LWPs as it

receives much more rainfall. Line 6, located in a zone of less rainfall than on Schofield Barracks, results in a thinner LWP.

Figure 15 is a conceptual model of how velocity data, well data, and saprolite alteration may interrelate. To prove these relationships, more research is needed. This study shows significant promise that such relationships may be established.

Conclusions

This study set out to investigate vital information concerning the depth and variability of the critical zone using the growing technique, MASW. The results proved promising as the MASW models accurately described the depth of the critical zones and showed potential variations caused by textural differences between flow types. These results are important because they expand the common use of MASW beyond typical geotechnical and engineering applications to investigating geologic problems. The specific geologic question addressed in this study is the rate of advancement of the weathering front and how it relates to climate variations. These questions were successfully addressed using MASW.

The study also furthered the technology of MASW with new experiment designed that improve the quality and confidence of the shear wave velocity models. These technological advances will be valuable to future studies where limitations have prevented MASW from obtaining needed data. The proof of technique established in this paper for the seismic investigation of weathering, is likely to apply to other Hawaiian islands where weathering rates and ground stability are vital information.

This method can also be expanded to the study of weathering in other basaltic regions and potentially to other geologic environments. MASW should be in greater consideration as a

valuable tool to engineers and geoscientists to map the subsurface in order to address multiple engineering and geologic questions.

References

Banab, K. K. and Motazdian, D., 2010, On the efficiency of the Multi-Channel Analysis of Surface Wave method for shallow and semideep loose soil layers: International Journal of Geophysics Volume 2010, Article ID 403016.

Beaulieu, C., Sarmiento, S. E., Fletcher, M., Chen, J., and Medvigy, D., 2012, Identification and characterization of abrupt changes in land uptake of carbon: Global Biogeochemical Cycles [0886-6236], v. 26.

Beaulieu, E., Godderis, Y., Labat, D., Roelandt, C., Oliva, P., and Guerrero, B., 2010, Impact of atmospheric CO2 levels on continental silicate weathering: Geochemistry Geophysics Geosystems, v. 11, n. 7.

Bell, R. W. and Ho, G. E., 1996, Workshop on the restoration and management of mined lands: Principles and Practice: 8-13 December, Guangzhou, China.

Boiero, D., Wiarda, E., and Vermeer, P., 2013, Surface-and guided-wave inversion for near-surface modeling land and shallow marine seismic data: The Leading Edge, June 2013, v. 32, p. 634-637.

Carnevale, M., Hager, J., Brinkmann, J. W., and Jones, B. R., 2005, MASW and GPR survey to delineate depth to bedrock and crystal cavities for mineral exploration: Proceedings of the Symposium on the Application of Geophysics to Engineering and Environmental Problems, p. 1051-1060.

Chandrakaran, S. and Nambiar, M.R.M., 1993, Role of iron oxide on shear strength behavior of latentic Soils: Indian Geotechnical Journal, (24), I, 195-207.

Cohen, A.S., Coe, A.L., Harding, S.M., and Schwark, L., 2004, Osmium isotope evidence for the regulation of atmospheric CO2 by continental weathering: Geology, v.32, p. 157–160.

Dalvi, A.D., Bacon, W.G., and Osborne, R.C., 2004, The past and the future of nickel laterites, in PDAC 2004 International Conference Trade Show and Investors Exchange, Toronto, Canada, March 7–10, 2004, Proceedings: Toronto, Canada, Prospectors and Developers Association of Canada, 27 p.

Dessert, C., Dupre B., Gaillardet J., Francois L.M., and Allegre C.J., 2003, Basalt weathering laws and the impact of basalt weathering on the global carbon cycle: Chemical Geology, v. 202, p. 257–273.

Dixon, J. L., Heimsath, A. M., Amundson, R., 2009, The critical role of climate and saprolite weathering in landscape evolution: Earth Surface Processes and Landforms, v. 34(11), p. 1507-1521.

Eker, A. M., Akgün, H., and Koçkar, M. K., 2012, Local site characterization and seismic zonation study by utilizing active and passive surface wave methods: A case study for the northern side of Ankara, Turkey: Engineering Geology, v. 151, p. 64–81.

Ferrier, K. L., Perron, J. T., Mukhopadhyay, S., Rosener, M., Stock., J. D., Huppert, K. L., and Slosber, M., 2013, Covariation of climate and long-term erosion rates across steep rainfall gradient on the Hawaiian island of Kaua'i: Geological Society of America, v. 125, p. 1146-1163.

Freyssinet, P., Butt, C.R.M., Morris, R.C., and Piantone, P., 2005, Ore-forming processes related to lateritic weathering: Economic Geology 100th Anniversary Volume, p. 681–722.

Gleeson, S.A., Butt, C.R.M., and Elias, M., 2003, Nickel laterites, a review: SEG Newsletter, v. 54, p. 11–18.

R.J., Marsh, E. E., and Monecke, T., eds., The challenge of finding new mineral resources—Global metallogeny, innovative exploration, and new discoveries: Society of Economic Geologists Special Publication 15, p. 451–485.

Goudie, A. S., and Viles, H. A., 2012, Weathering and the global carbon cycle: Geomorphological perspectives: Earth-Science Reviews, v. 113(1-2), p. 59-71.

Gui, M. and Yu, C., 2008, Rate of strength increase of unsaturated lateritic soil: Canadian Geotechnical Journal, v. 45, p. 1335-1343.

Hilley, G.E., Chamberlain, C.P., Moon, S., Porder, S., and Willett, S.D., 2010 Competition between erosion and reaction kinetics in controlling silicate-weathering rates: Earth and Planetary Science Letters, v. 293, p. 191–199.

Hilley, G.E. and Porder, S., 2008. A framework for predicting global silicate weathering and CO2 drawdown rates over geological time-scales: Proceedings of the National Academy of Sciences, v. 105(44), p. 16855–16859.

Karray, M., Lefebvre, G., Ethier, Y., Bigras, A., 2010, Assessment of deep compaction of the Peribonka dam foundation using “modal analysis of surface waves” (MASW): Canadian Geotechnical Journal, v. 47, p. 312-326.

Kashiwagi, H., Ogawa, Y., Shikazono, N., 2008, Relationship between weathering, mountain uplift, and climate during the Cenozoic as deduced from the global carbon-strontium model: Palaeogeography, Palaeoclimatology, Palaeoecology, v. 270, p. 139-149.

Kaufmann, R. D., Xia, J., Benson, R. C., Yuhr, L. B., Castro, D. W., Park, C. B., 2005, Evaluation of MASW data acquired with a hydrophone streamer in a shallow marine environment: Journal of Environment and Engineering Geophyics, v. 10, p. 87-98.

Kump, L., Brantley, S.L., and Arthur, M., 2000. Chemical weathering, atmospheric CO2, and climate. Annu. Rev. Earth Planet. Sci., v. 28, p. 611–667.

Laskou, M., and Economou-Eliopoulos, M., 2013, Bio-mineralization and potential biogeochemical processes in bauxite deposits: genetic and ore quality significance: Mineralogy and Petrology, v. 107, p. 471-486.

Lau L.C. and Mink J.F., 2006, Hydrology of the Hawaiian Islands: University of Hawaii Press.

Lenton, T. M. and Britton, C., 2006, Enhanced carbonate and silicate weathering accelerates recovery from fossil fuul CO2 perturbations: Global Biogeochemical Cycles, v. 20(3).

Mahajan, A. K. and Rai, N, 2011, Using MASW to map depth to bedrock underneath Dehradun fan deposits in NW Himalay: Current Science, v. 100, p. 233-238.

Marsh, E.E. and Anderson, E.D., 2011, Ni-Co laterite deposits: U.S. Geological Survey Open-File Report 2011–1259.

Meyer, F. M., Happel, U., Hausberg, J., Wiechowski, A., 2002, The geometry and anatomy of the Los Pijiguaos bauxite deposit, Venezuela: Ore Geology Review, v. 20, p. 27-54.

Miller, R.D., Xia, J., Park, C.B., and Ivanov J.M, 1999, Multichannel analysis of surface waves to map bedrock: The Leading Edge, v. 18, p. 1392–1396.

Montomery, D. R., Brandon, M. T., 2002, Topographic controls on erosion rates in tectonically active mountain ranges: Earth Planet Science, v. 201, p. 481-489.

Nelson, S. T., Tingey, D. G., and Selck, B., 2013, The denudation of ocean islands by ground and surface waters: The effects of climate, soil thickness, and water contact times on Oahu, Hawaii: Geochimica et Cosmochimica Acta 103 (2013) p. 276-294.

Park, C., 2013, MASW for geotechnical site investigation: The Leading Edge, June 2013, v. 32, p. 656-662.

Park, C.B., 2008, Imaging dispersion of passive surface waves with active scheme: Symposium on the Application of Geophysics to Engineering and Environmental Problems (SAGEEP 2008), Philadelphia, April 6-10, Proceedings on CD Rom.

Park, C.B., and Carnevale, M., 2010, Optimum MASW survey - revisit after a decade of use: Geo-Institute Ann. Mtng (GeoFlorida 2010), February 20-24, 2010, West Palm Beach, FL.

Park, C.B. and Miller, R. D., 2008, Roadside passive multi-channel analysis of surface waves (MASW): Journal of Environmental and Engineering Geophysics, v. 13, p. 1–11.

Park, C.B., Miller, R.D., and Xia J., 1999 Multichannel analysis of surface waves MASW: Geophysics, v. 64, p. 800–808.

Park, C.B., and Shawver, J.B., 2009, MASW survey using multiple source offsets: Proceedings of the Symposium on the Application of Geophysics to Engineering and Environmental Problems, Fort Worth, TX, March 29-April 2, 2009.

Patterson, S. H., 1967, Bauxite reserves and potential aluminum resource of the world: Geological Survey, Library of Congress catalog-card No. GB 67-156.

Pearson, P.N. and Palmer, M.R., 2000, Atmospheric carbon dioxide concentrations over the past 60 million years: Nature, v.406, p. 695–699.

Porder, S., Hilley, G.E., and Chadwick, O.A., 2007 Chemical weathering, mass loss, and dust inputs across a climate by time matrix in the Hawaiian Islands: Earth Planetary Science, Lett. 258, p. 414–427.

Raymo, M.E., 1991, Geochemical evidence supporting T.C. Chamberlin's theory of glaciations: Geology, v.19, p. 344–347.

Sadleir, S. B., and Gilkes, R. J., 1976, Development of bauxite in relation to parent material near Jarrahdal, Western Australia: Journal of the Geological Society of Australia, v. 23, p. 334-344.

Sherrod D. R., Sinton J. M., Watkins S. E., and Brunt K. M, 2007, Geologic 796 map of the State of Hawai'i. 797 OF 2007-1089, 85.

Sirles, P., Sheehan, J., and Pendrigh, N., 2013, Passive near-surface seismic data where all else falls: Leading Edge special section: Urban Geophysics, March 2013, p. 308-314.

Suto, K., 2013, MASW surveys in landfill sites in Australia: The Leading Edge, June 2013, v. 32, p. 674-678.

Trupti, S., Srinivas, K.N.S.S.S, Kishore, P. P., Seshunarayana, T., 2012, Site characterization studies along coastal Andhra Pradesh-India using multichannel analysis of surface waves: Journal of Applied Geophysics, v. 79, p. 82-89.

Ulery, A.L. and Drees, L.R., 2008, Methods of soil analysis: Part 5 – Mineralogical methods: Soil Science Society of America, Inc., Madison, Wisconsin, p. 544.

Watabe, Y. and Sassa, S., 2008, Application of MASW technology to identification of tidal flat stratigraphy and its geoenvironmental interpretation: Marine Geology, v. 252, p. 79-88.

West J. A., 2012, Thickness of the chemical weathering zone and implications for erosional and climatic drivers of weathering and for carbon-cycle feedbacks: Geology, v. 40, p. 811–814.

Wilson M. J., 2004, Weathering of the primary rock-forming minerals: processes, products and rates: Clay Minerals, v. 39, p. 233–266.

Xia, J., Miller, R. D., Park, C. B., Hunter, J. A., Harris, J. B., and Ivanov J., 2002, Comparing shear-wave velocity profiles inverted from multi-channel surface wave with borehole measurements: Soil Dynamics and Earthquake Engineering, v. 22(3) p. 181–190.

Xia, J., Miller, R.D., Park, C.B., 1999, Estimation of near-surface shear-wave velocity by inversion of Rayleigh waves: Geophysics, v. 64(3), p. 691-700.

Younge, O. R. and Moomaw, J.C., (1960), Revegetation of Stripmined Bauxite Land in Hawaii: Economic Botany, v. 14, p. 316-330.

Xu, C. and Butt, S. D., 2006, Evaluation of MASW techniques to image steeply dipping cavities in laterally inhomogeneous terrain: Journal of Applied Geophysics, v. 59, p. 106-116.

Zachos, J.C. and Kump, L.R., 2005, Carbon cycle feedbacks and the initiation of Antarctic glaciation in the earliest Oligocene: Global and Planetary Change, v. 47, p. 51–66.

Zeng, C., Xia, J., Miller, R. D., Tsoflias, G. P., and Wang, Z., 2012, Numerical investigation of MASW applications in presence of surface topography: Journal of Applied Geophysics, v. 84, p. 52-60.

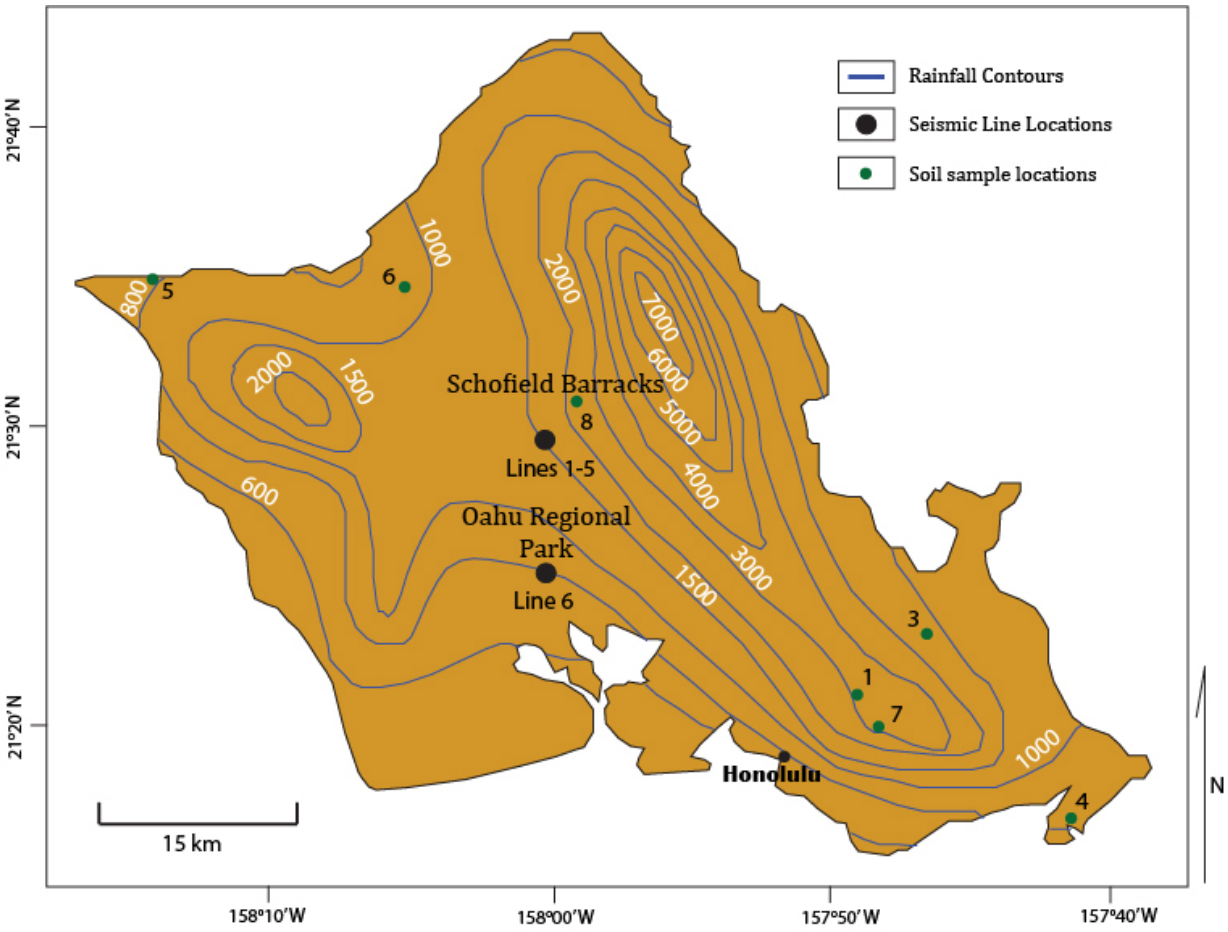

Figure 1. Index map of Oahu showing seismic profile locations, well locations, and precipitation contours representing mean annual rainfall in mm.

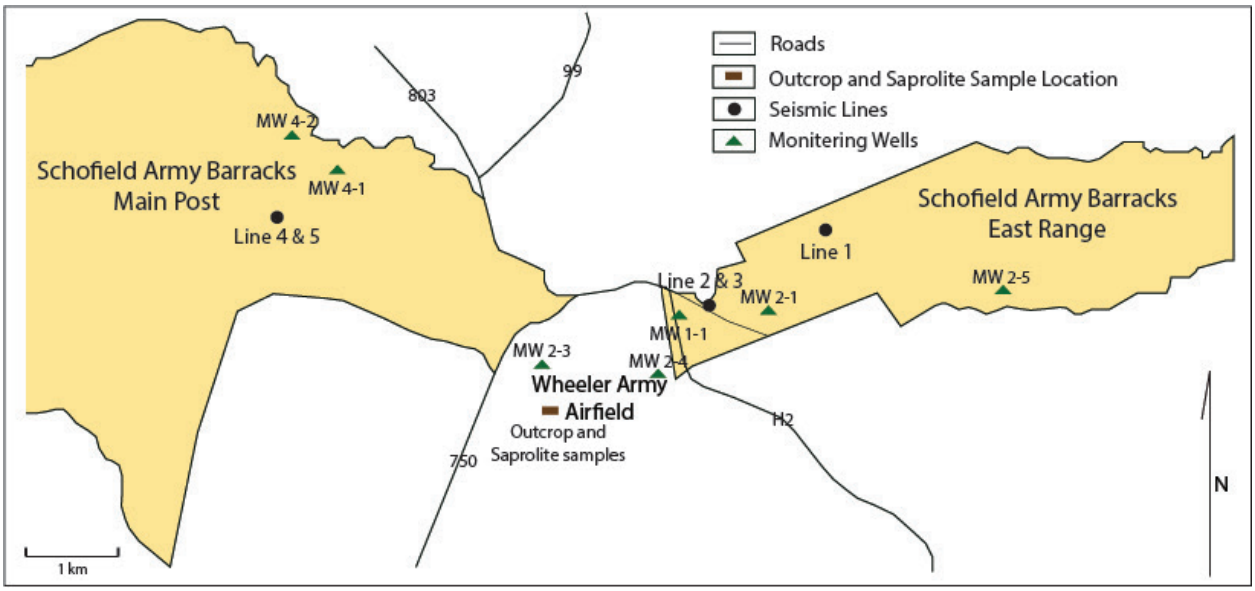

Figure 2. Index Map of Schofield Barracks showing well locations, seismic profile locations, and outcrop location.

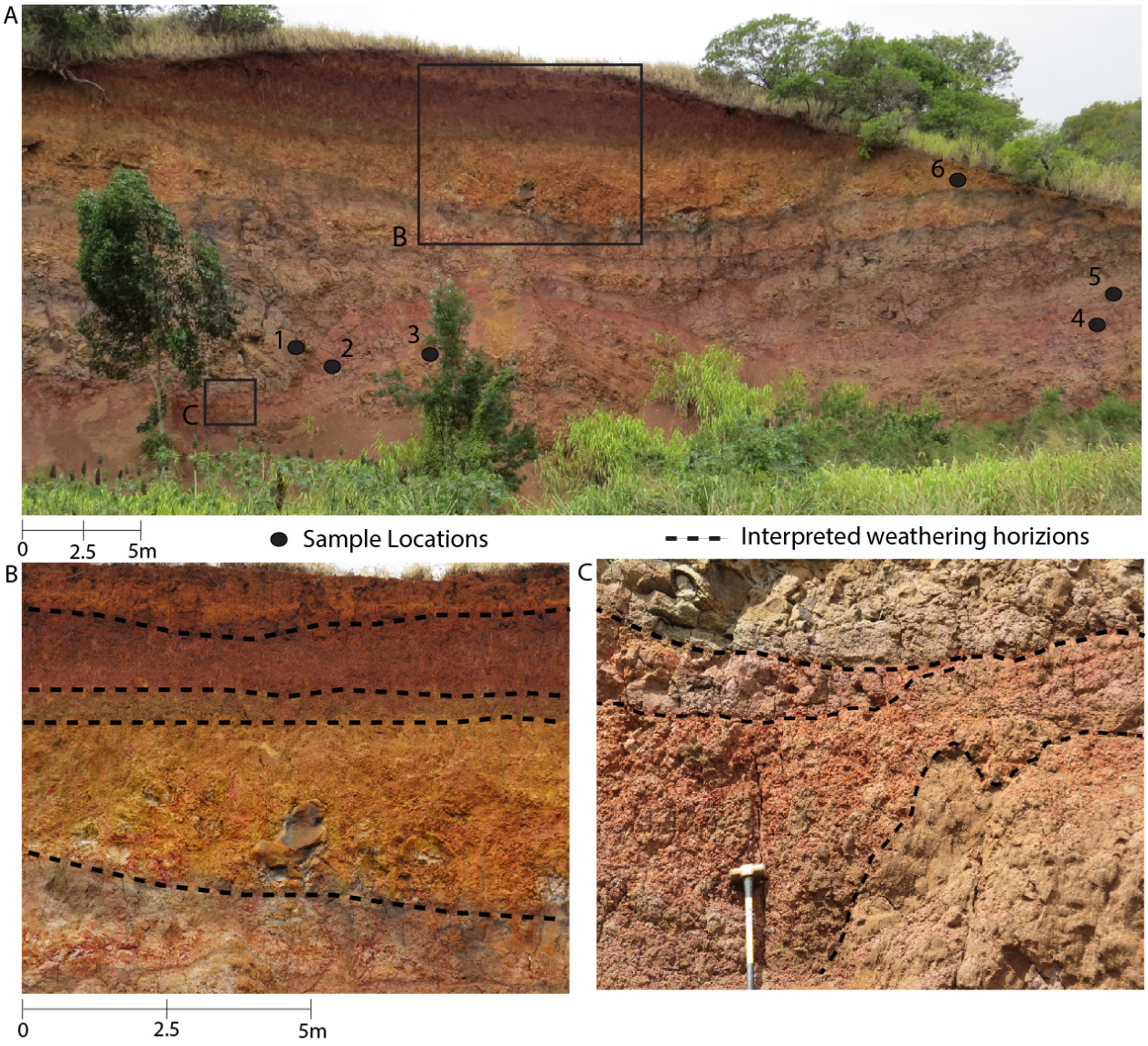

Figure 3. (A) Exposed outcrop cut by an old army runway on Wheeler Army Airfield (location on fig.2). Labeled dots 1-6 represent sample locations. B and C show zoomed in views of the weathering zone. Interpreted weathering horizons were based on color and changes in rigidity, and demonstrate the variability that can occur in a short distance both laterally and vertically.

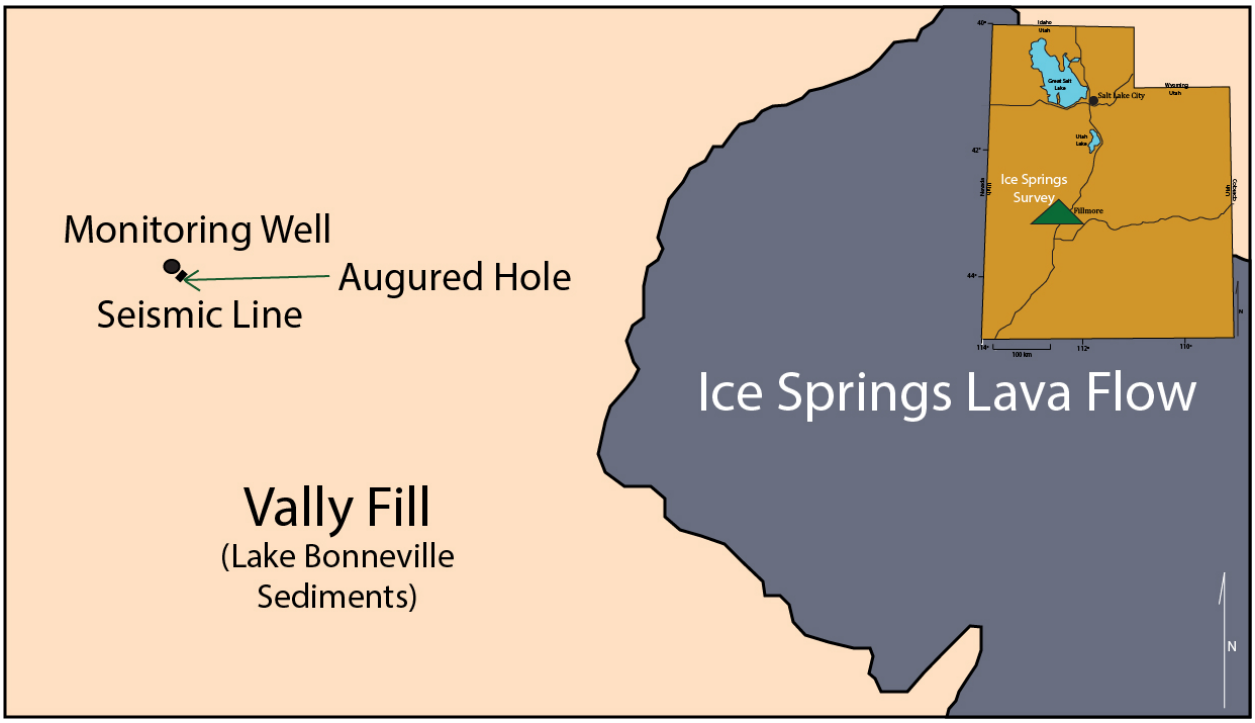

Figure 4. Index map of the Ice Springs location near Fillmore, Utah showing the seismic profile location, the monitoring well location, and the augured hole location.

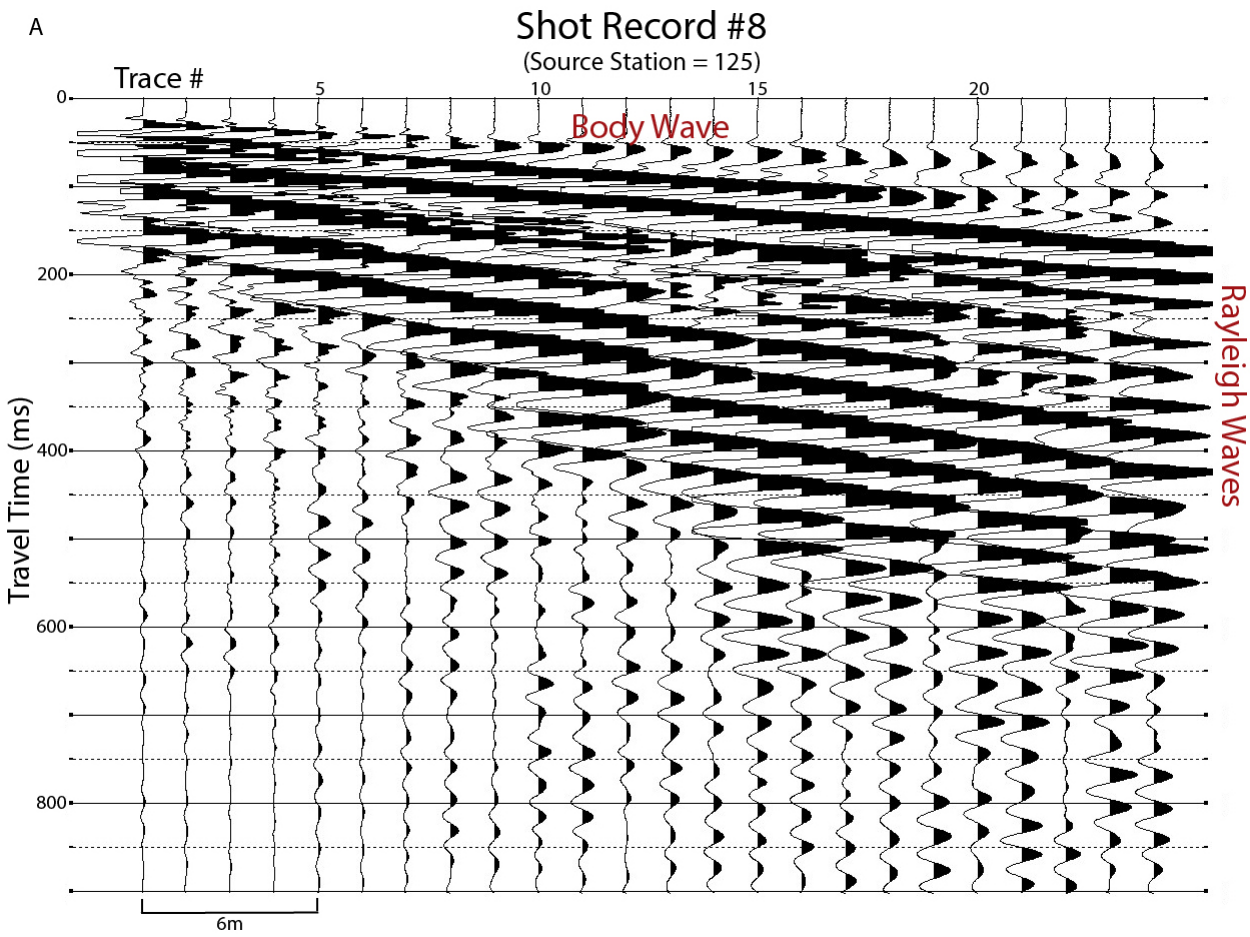

Figure 5. (A) Shot record from the Ice Springs line towards the SW of the profile, record #8. Data location labeled on Figure 8.

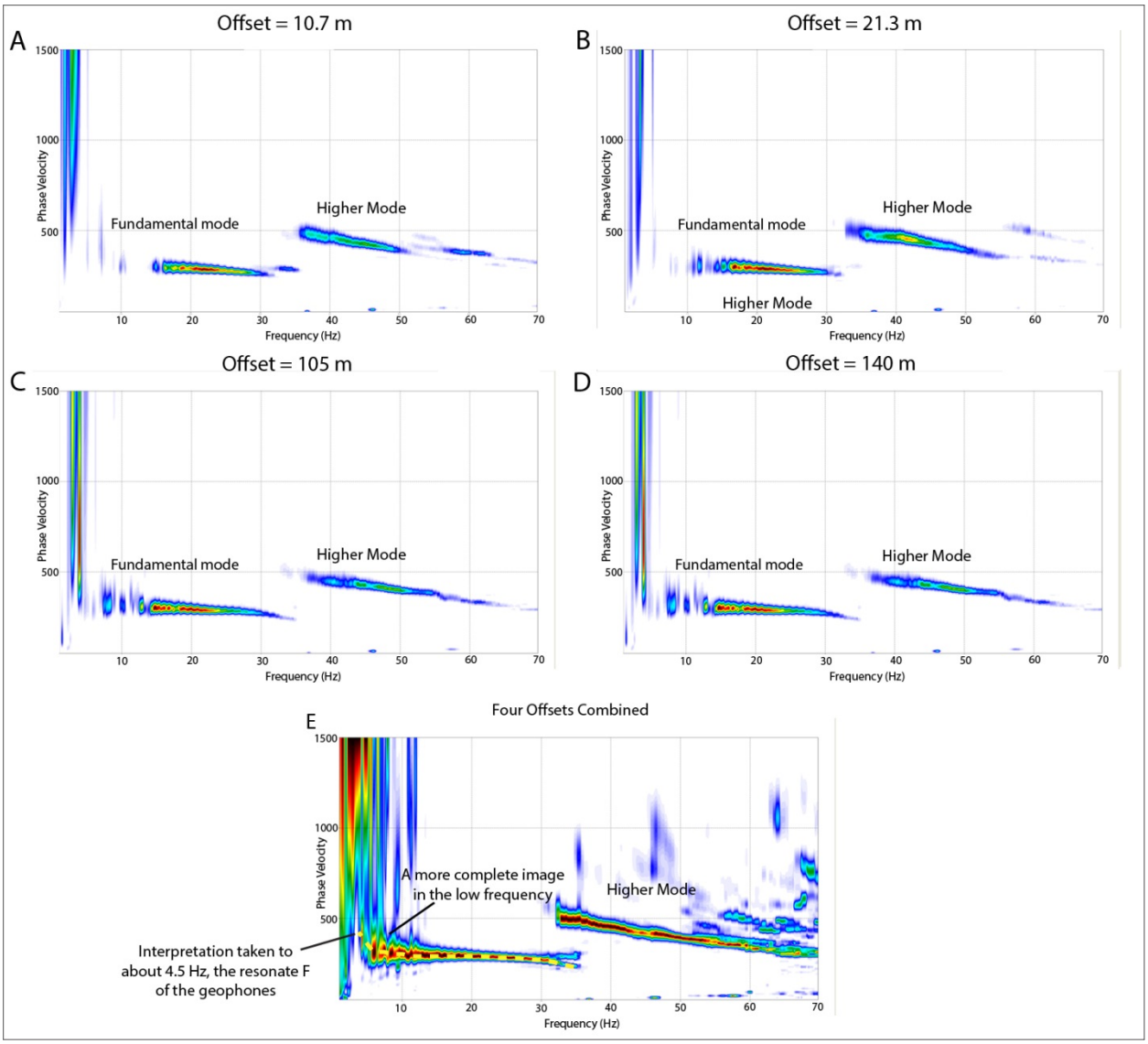

Figure 6: (A-D) Comparision of OT curves for individual experiments at offsets of a) 10.7 m, b) 21.3 m, c) 32 m, d) 42.7 m. (E) The combination of all four individual experiments into one OT images showing the dramatic image quality improvement in the low frequency domain. Dispersion curve was interpreted down to about 4.5 Hz, the resonate frequency of the geophones.

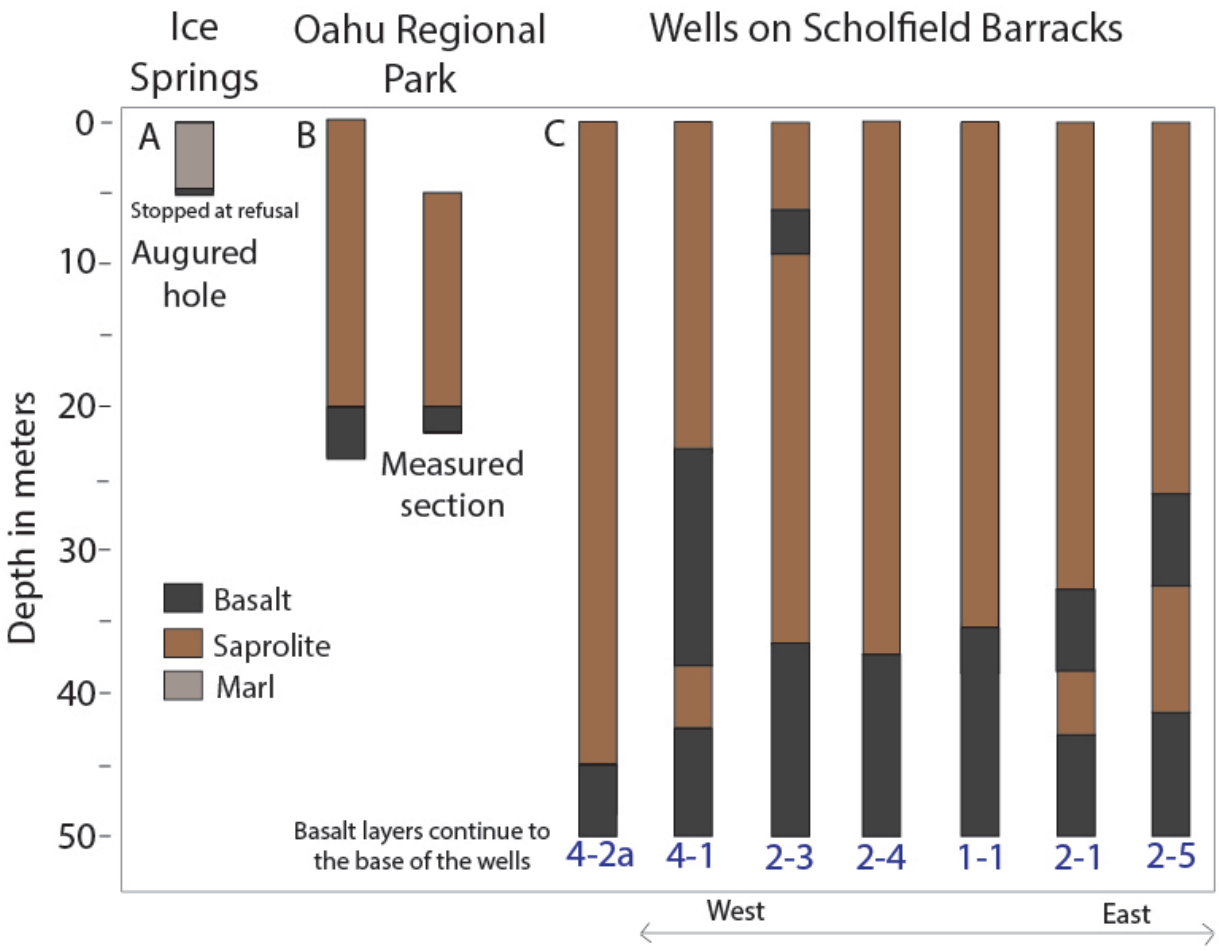

Figure 7. (A) Hand augured hole along the seismic line at Ice Springs showing marl down to 5m and then hard basalt. See fig. 4 (B) Well data near Oahu Regional Park showing a depth to basalt at 20m. Also a measured section along a highway road cut down to basalt at ~20m. See fig. 2. (C) Wells located on Scholfield Barracks trending west to east showing variations in saprolite and depths to basalt. See fig. 3 Basalt continues below shown depths.

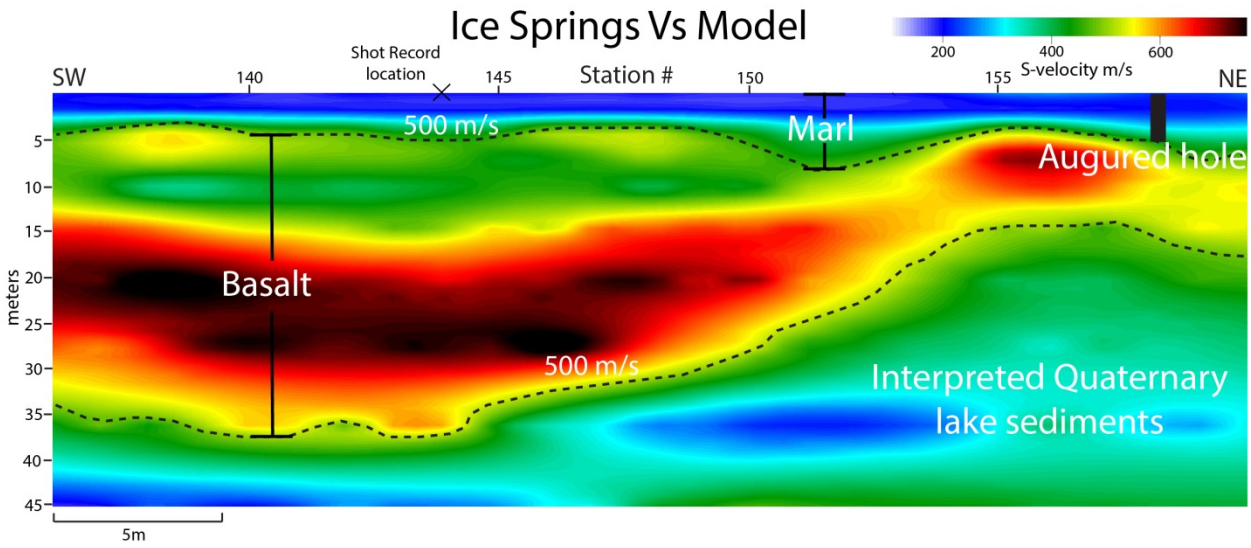

Figure 8. Velocity model for the active survey at the reference site at Ice Springs, UT. The hand augured hole strongly correlates with the interpreted depth from the seismic data at a velocity of ~500m/s as shown on the model between 4-6m. The base of the lava flow is interpreted and varies significantly, which is in agreement with the geologic environment. Quaternary sediments below the lava flow are likely to be found beneath the lave flow. See fig. 7

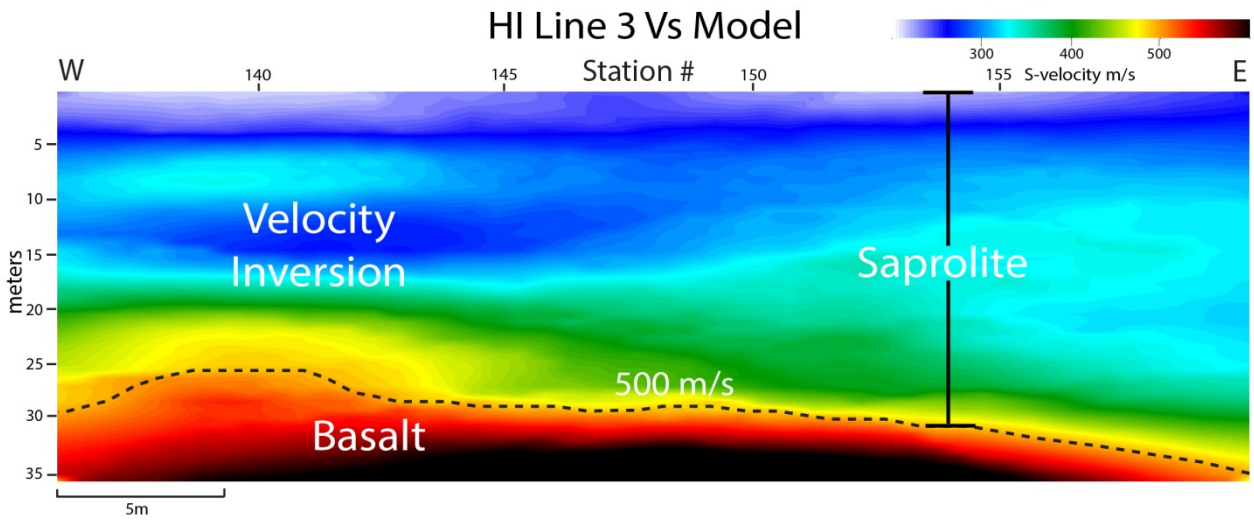

Figure 9. Velocity model for active survey line 3, Oahu, HI. Interpreted saprolite/bedrock boundary is shown to vary between 26 and 34m marked by the 500 m/s contour. These depths are shallower than local well data, 1-1 being about 300m away, but still within reason of expected variations. Velocity inversions seen are likely in response to weathering variability. See fig. 7

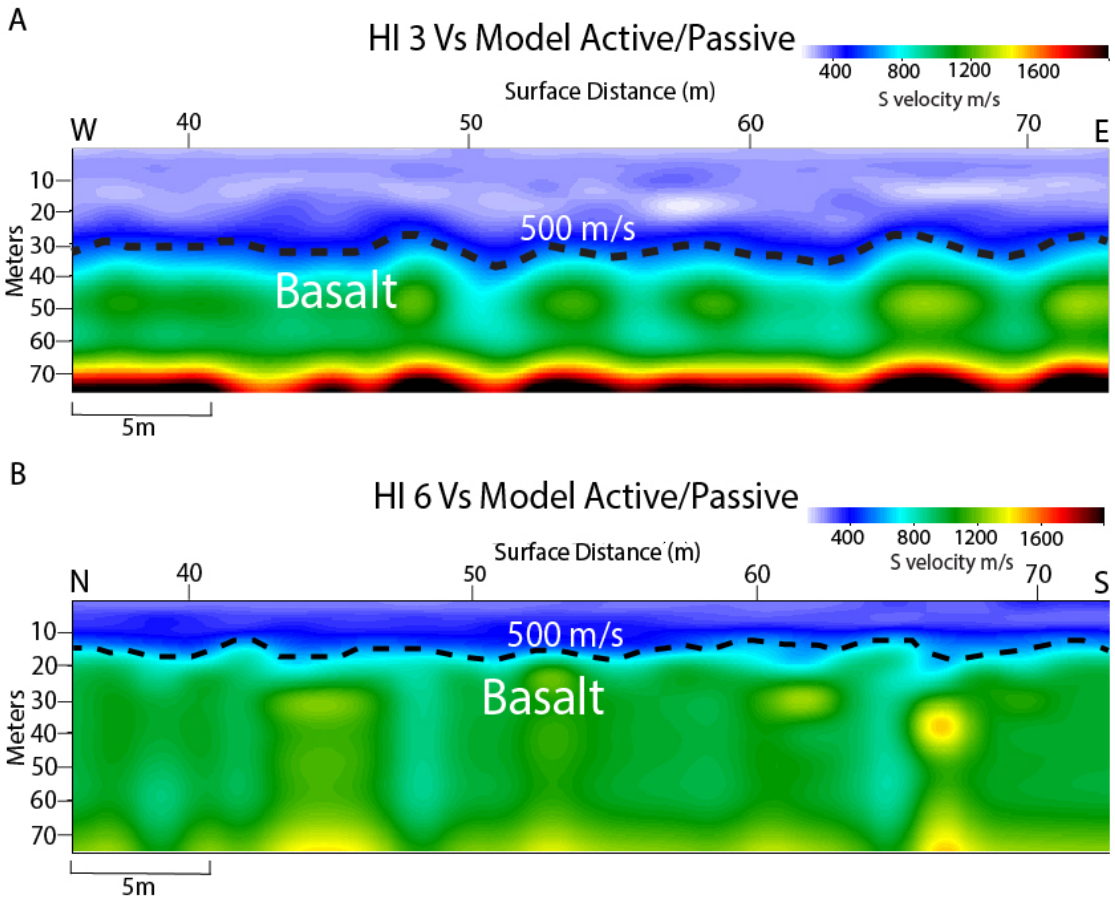

Figure 10. (A) Velocity model derived from the active/passive method showing a significant increase in the depth of investigation at site 3. Compare to fig. 9. The 500m/s contour marks the interpreted depth to basalt and correlates well with the first model on figure 9 and the expect range shown by well data across the barracks.(B) Velocity model derived from the active/passive method showing a significant increase in the depth of investigation at site 6 . The basalt boundary marked by the 500m/s contour between 15-20m correlates well with data from figures 7 and 11.

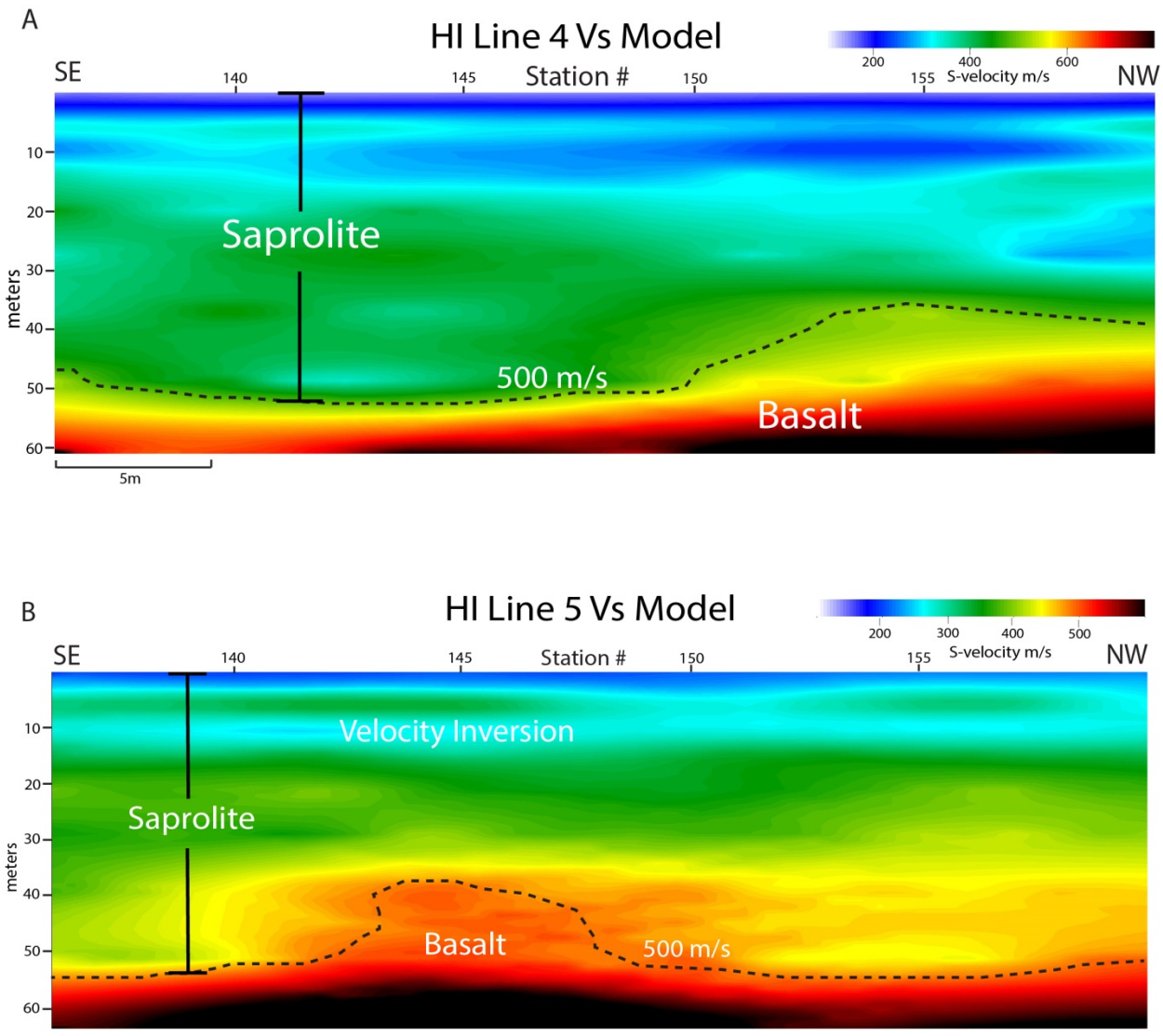

Figure 11. Velocity models for active survey lines 4 and 5, Oahu, HI. These lines are located ~100m apart showing similar depth to bedrock but with significant variability between 40-55m. Bedrock depth is interpreted at a 500 m/s contour. These depths correlate with the expected depths based on well data across the barracks. See fig. 7

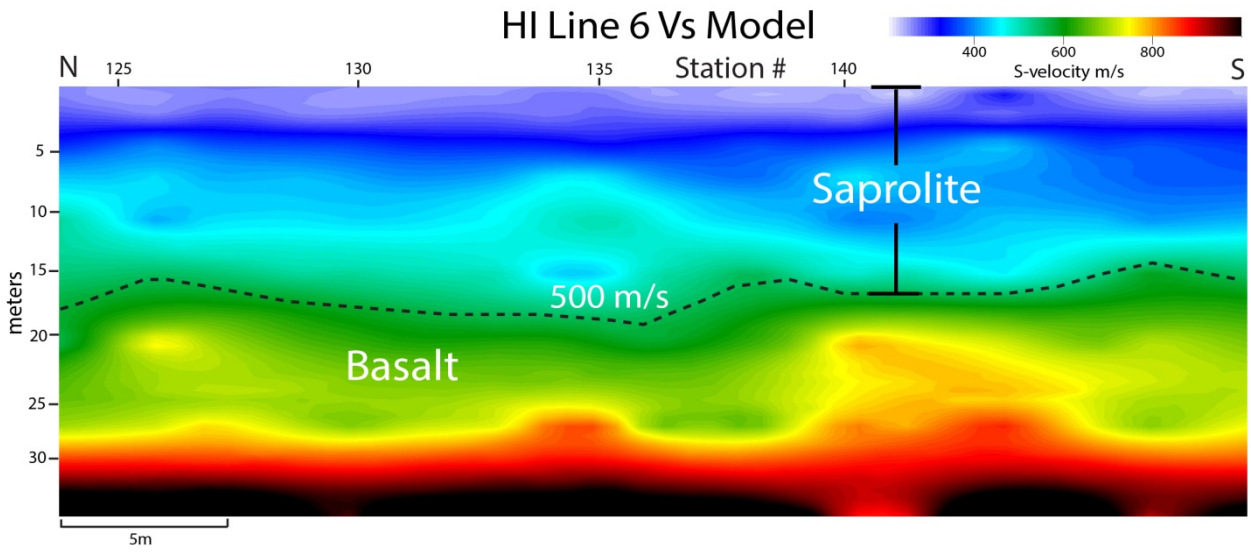

Figure 12. Active survey line 6 located at the Oahu Regional Park, HI. Interpreted saprolite/basalt boundary marked by a 500m/s contour between 15-20m. Data are strongly correlated with well data and measure section seen on figure 7.

Location	Well # /MASW Profile	Depth to Bedrock	Weathering Rate for Youngest Age (1.8 Ma)	Weathering Rate for Oldest Age (3.2 Ma)
Schofield Barracks	4-2a	45 m	0.025 m/ka	0.014 m/ka
	4-1	42 m	0.023 m/ka	0.013 m/ka
	2-3	39 m	0.022 m/ka	0.012 m/ka
	2-4	40 m	0.022 m/ka	0.012 m/ka
	1-1	36 m	0.020 m/ka	0.011 m/ka
	2-1	38 m	0.021 m/ka	0.012 m/ka
	2-5	36 m	0.020 m/ka	0.011 m/ka
	Line 3	26 - 35 m	0.019 m/ka	0.011 m/ka
	Line 4	36 - 52 m	0.029 m/ka	0.016 m/ka
	Line 5	38 - 54 m	0.030 m/ka	0.017 m/ka
Mink Park	Measured Section	21 m	0.012 m/ka	0.007 m/ka
	Well log	20 m	0.011 m/ka	0.006 m/ka
	Line 6	20-24 m	0.013 m/ka	0.008 m/ka

Table 1. Rates of the advancement of the weathering front based on wells, measured section, and seismic data.

a

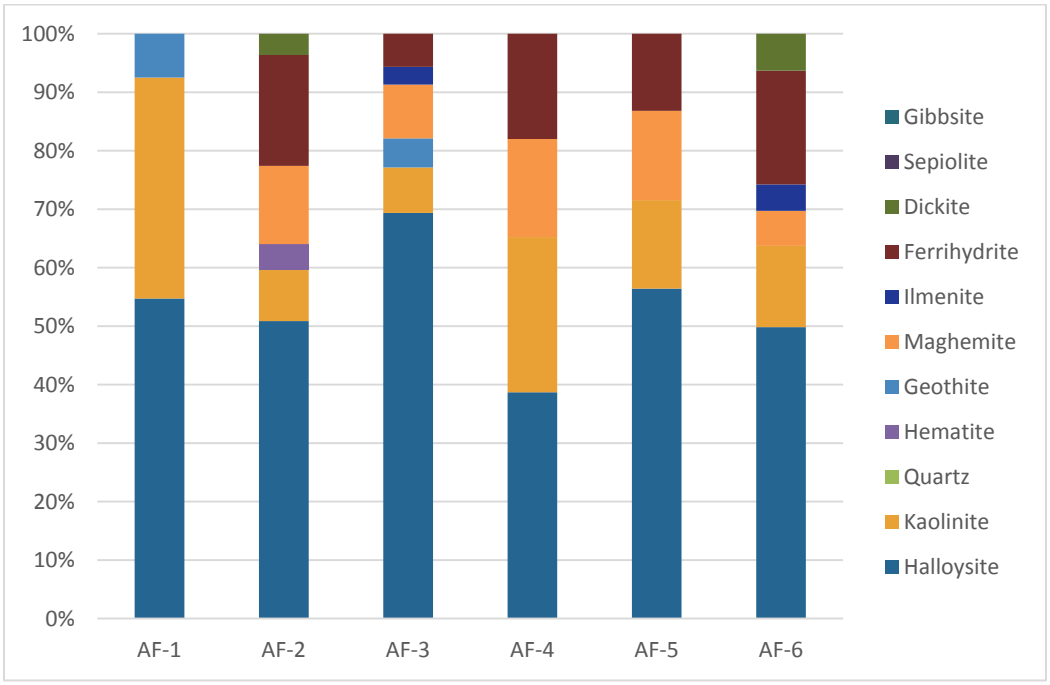

b

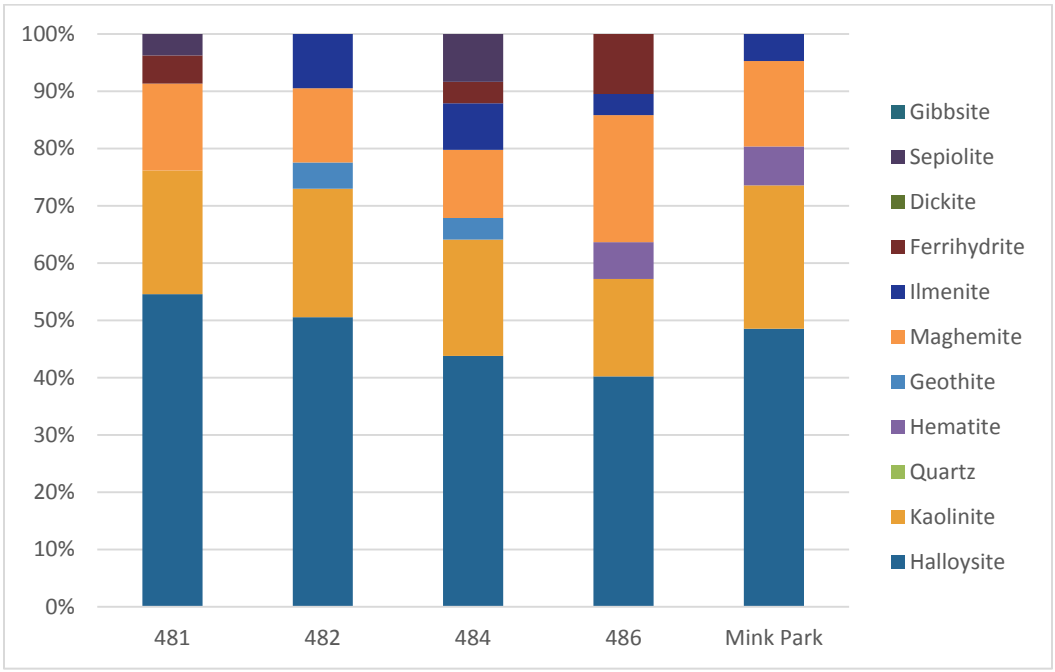

Figure 13. a) Mineralogy for samples located at the airfield on Schofield Barracks (fig. 3). b) Mineralogy for samples at the dryer Mink Park location.

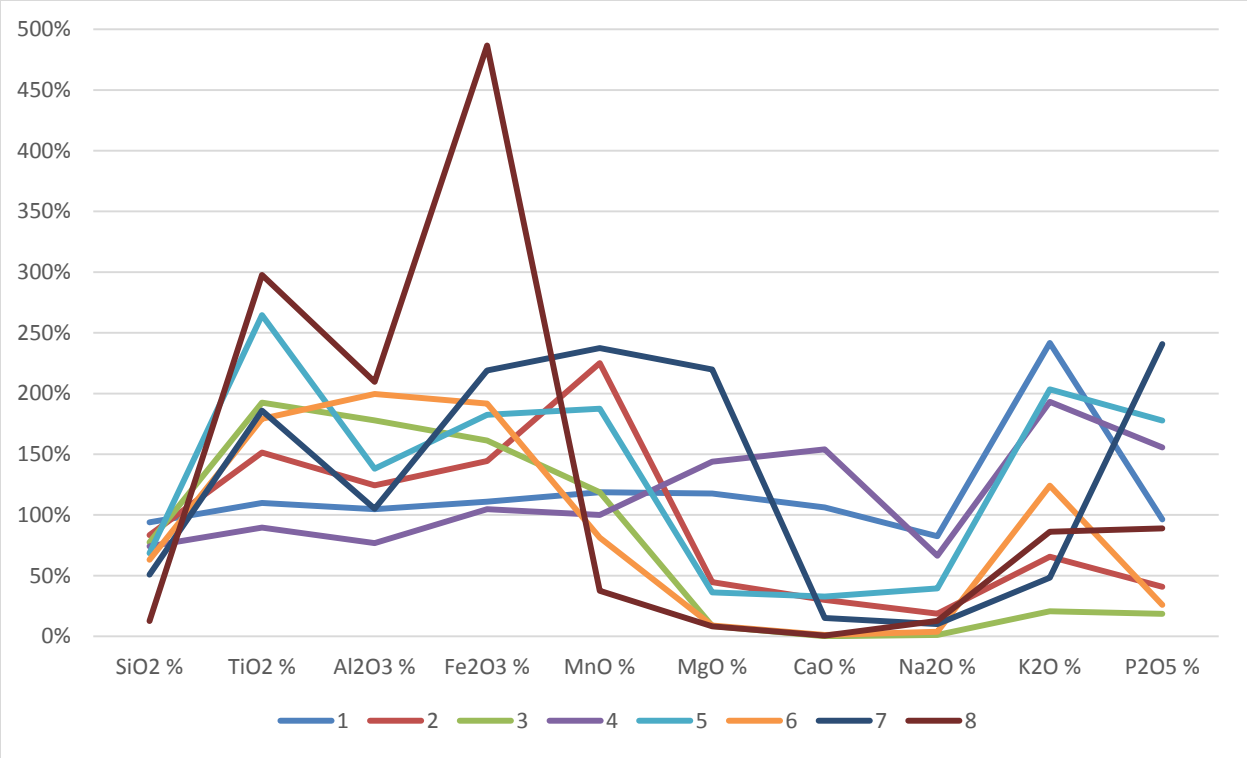

Figure 14. Major element analysis for surface samples under various climate conditions (fig. 1).

Enrichment trends indicate leaching of Mg, Ca, and Na while concentrating Ti, Al, and Fe.

Sample	SiO2	TiO2	Al2O3	Fe2O3	MnO	MgO	CaO	Na2O	K2O	P2O5	LOI	Total
HWN-68	52.43	2.12	14.14	11.49	0.16	6.39	9.63	2.68	0.29	0.27	-0.12	99.47
slight												
1	49.23	2.33	14.80	12.75	0.19	7.52	10.23	2.21	0.12	0.26	0.24	99.88
2	43.71	3.21	17.58	16.59	0.36	2.85	2.89	0.50	0.19	0.11	11.87	99.85
3	40.57	4.08	25.16	18.53	0.19	0.54	0.01	0.03	0.06	0.05	10.72	99.94
moderate												
4	38.91	1.90	10.86	12.03	0.16	9.19	14.83	1.78	0.56	0.42	9.14	99.78
5	35.92	5.61	19.53	20.97	0.30	2.31	3.15	1.06	0.59	0.48	9.95	99.86
6	33.04	3.80	28.23	22.03	0.13	0.57	0.11	0.10	0.36	0.07	11.43	99.87
7	26.62	3.94	14.86	25.16	0.38	14.04	1.45	0.27	0.14	1.65	11.14	99.64
severe												
8	10.68	8.81	24.20	33.03	0.11	0.28	0.07	0.02	0.42	0.18	22.05	99.86

Table 2. Major element analysis of basalt and soil/saprolite samples. Fe, Al, and Ti showing strong enrichment trends.

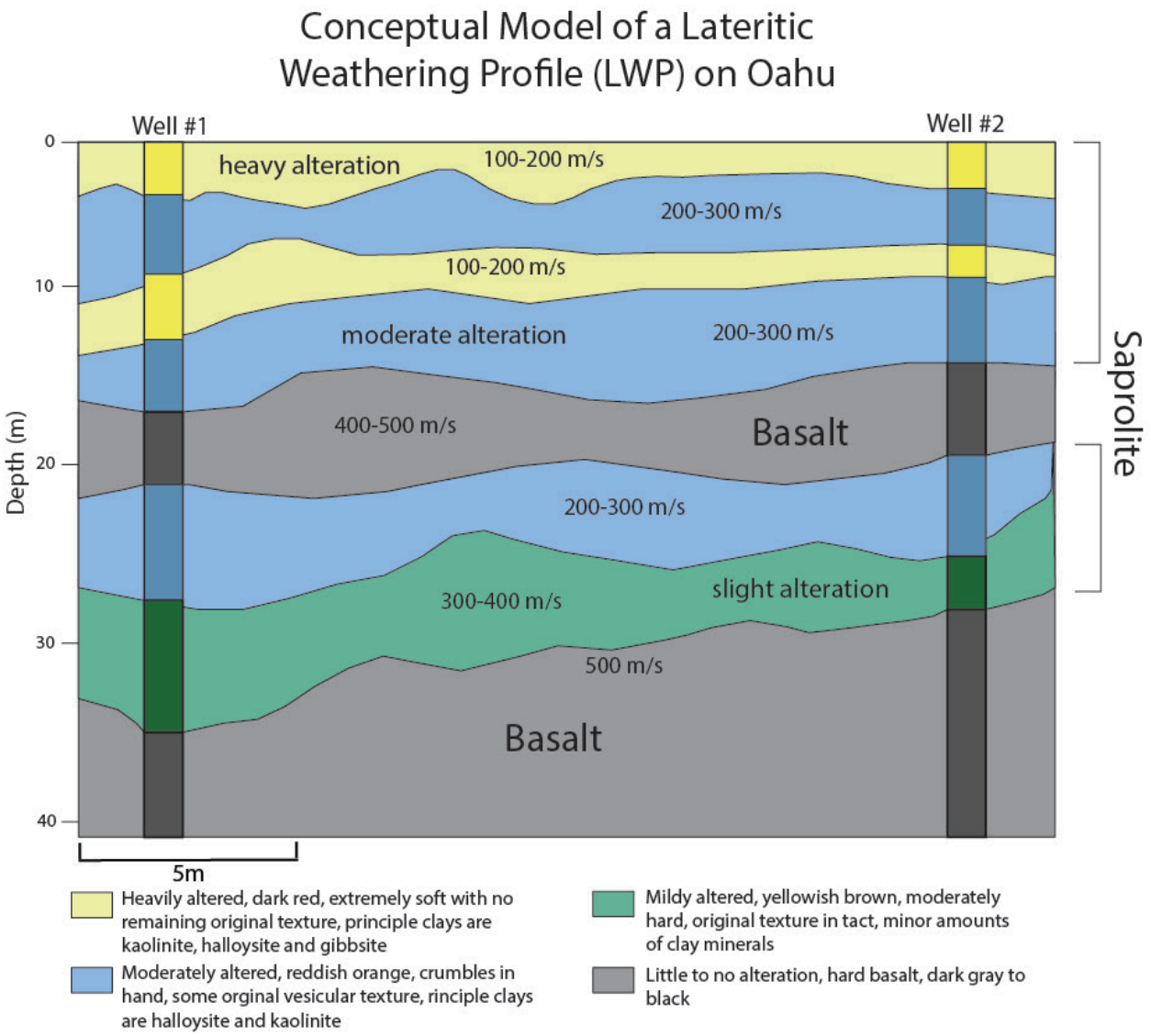

Figure 15. Conceptual Model showing expected shear-wave velocity and mineralogical heterogeneity within a lateritic weathering profile (LWP) on Oahu, HI. Colored zones represent a range of potential velocities corresponding to degrees of basaltic alteration in the saprolite.